Cardiovascular Research (2008) **77**, 371–379
doi:10.1093/cvr/cvm001

Dyslipidaemia in type II diabetic mice does not aggravate contractile impairment but increases ventricular stiffness

An Van den Bergh[1], Annelies Vanderper[1], Peter Vangheluwe[2], Fanny Desjardins[3], Ines Nevelsteen[1], Wim Verreth[4], Frank Wuytack[2], Paul Holvoet[4], Willem Flameng[1], Jean-Luc Balligand[3], and Paul Herijgers[1]*

[1]*Laboratory of Experimental Cardiac Surgery, Department of Cardiovascular Disease, Katholieke Universiteit Leuven, Provisorium I, Minderbroedersstraat 19, K.U.Leuven postbus 01033 – FEHA, 3000 Leuven, Belgium;* [2]*Laboratory of Physiology, Katholieke Universiteit Leuven, Leuven, Belgium;* [3]*Department of Medicine, Unit of Pharmacology and Therapeutics, Université Catholique de Louvain, Belgium; and* [4]*Department of Cardiovascular Diseases, Atherosclerosis and Metabolism Unit, Katholieke Universiteit Leuven, Leuven, Belgium*

Received 17 April 2007; received in revised form 11 July 2007; accepted 17 July 2007; online publish-ahead-of-print 14 August 2007

Time for primary review: 22 days

KEYWORDS
Apoptosis;
Athcrosclcrosis;
Contractile function;
Diabetes;
SR (function)

Aims Type II diabetes, often associated with abdominal obesity, frequently leads to heart failure. Clinical and epidemiological evidence suggests that supplemental dyslipidaemia and hypertension, as clustered in the metabolic syndrome, aggravate the cardiovascular outcome. The differential impact of type II diabetes and the metabolic syndrome on left ventricular function, however, remains incompletely defined.
Methods and results We studied left ventricular function *in vivo* using pressure–volume analysis in obese diabetic mice with leptin deficiency (ob/ob) and obese diabetic dyslipidemic mice with combined leptin and low-density lipoprotein-receptor deficiency (DKO). ob/ob and DKO mice developed a diabetic cardiomyopathy, characterized by impaired contractility and relaxation, from the age of 24 weeks onwards. This was—at least partially—explained by increased apoptosis and disturbed Ca^{2+} reuptake in the sarcoplasmic reticulum (SR) in both mouse models. DKO, but not ob/ob, developed increased end-diastolic ventricular stiffness, paralleled by increased left ventricular myocardial fibrosis. Cardiac output was preserved in ob/ob mice by favourable loading conditions, whereas it decreased in DKO mice.
Conclusions Type II diabetes in mice leads to impaired contractility and relaxation due to disturbed Ca^{2+} reuptake in the SR, but only when dyslipidaemia and hypertension are superimposed does vascular–ventricular stiffening increase and left ventricular myocardial fibrosis develop.

1. Introduction

Patients with type II diabetes are at increased risk of developing heart failure.[1] The existence of a primary diabetic cardiomyopathy characterized by diastolic and/or systolic impairment was demonstrated before in type II diabetic mouse models.[2,3] In type II diabetic patients abdominal obesity, dyslipidaemia, and hypertension are known associated risk factors for the development of heart failure.[4] These 'metabolic syndrome' features promote atherosclerotic plaque formation and might additionally induce ischaemic heart disease.[5] In patients with the metabolic syndrome the relative contribution of the dyslipidemic/atherosclerotic component and the diabetes/obesity component in the development of heart failure is incompletely known. In the current study, we investigated cardiac contractility and haemodynamics in the single knockout leptin-deficient ob/ob mouse model for obesity and type II diabetes and in a double knockout (DKO) mouse model with combined deficiency of leptin and of the low-density lipoprotein receptor (LDLR) presenting the metabolic syndrome exhibiting type II diabetes, hypertension, obesity, dyslipidaemia, and atherosclerosis.[6,7] The development of haemodynamic alterations was studied at the age of 12, 24, and 36 weeks.

Increased cardiac myocyte apoptosis and depressed sarcoplasmic reticulum (SR) Ca^{2+} pump (SERCA2a) activity were associated with cardiac dysfunction in the ob/ob mouse model of type II diabetes and obesity.[8,9] Sustained dyslipidaemia is known to increase ceramide production, which trough nitric oxide formation causes apoptosis. Furthermore, SERCA activity is critically dependent on the membrane composition, which is in turn affected by the plasma lipid composition.[10,11] We hypothesised that in subjects

* Corresponding author. Tel: +32 16 337298; fax: +32 16 337855.
E-mail address: paul.herijgers@med.kuleuven.be

with the metabolic syndrome apoptosis and SERCA2a, dysfunction would be exacerbated. Therefore, we assessed the degree of apoptosis in the aforementioned single and double KO models. The expression of SERCA2a, its regulatory protein phospholamban (PLB), and its phosphorylation status were measured as well as SERCA2a activity.

2. Methods

2.1 Experimental animals

Experiments were conducted in C57BL/6J (WT) ($n = 67$), homozygous LDL receptor knockout mice ($LDLR^{-/-}$) ($n = 60$), ob/ob ($n = 46$), and DKO ($n = 51$) mice at 12, 24, or 36 weeks of age, of either sex. Mice were backcrossed for at least 10 generations into the C57BL/6J background and mice had 98.4% C57BL/6J background. $LDLR^{-/-}$, heterozygous ob/+, and C57BL/6J mice were purchased from Jackson Laboratory (Bar Harbor, ME, USA). Homozygous ob/ob and DKO mice were generated as described previously.[6] The investigation conforms with the *Guide for the Care and Use of Laboratory Animals* published by the US National Institutes of Health (NIH Publication No. 85-23, revised 1996).

2.2 Biochemical parameters

Blood of conscious mice was collected by tail bleeding into EDTA tubes after a 24 h fast. Plasma was obtained by centrifugation. Plasma insulin was determined with a mouse insulin ELISA (Mercodia), triglycerides and total cholesterol with a diagnostic reagent kit (Roche), and glucose with a glucometer (Menarini Diagnostics). Insulin resistance was calculated by a homeostasis model assessment (HOMA-IR) = fasting serum insulin (mU/L) times fasting blood glucose (mM)/22.5. To determine glucose tolerance, glucose was measured in samples obtained by tail bleeding before and 15, 30, 60, 120, 240, and 360 min after intraperitoneal glucose administration (20% glucose solution, 2 g/kg). The area under the curve (AUC) was used as a measure of glucose tolerance.

2.3 *In vivo* haemodynamic measurements

2.3.1 Left-ventricular pressure–volume analysis

The metabolic syndrome is associated with hypertrophy and alterations in pre- and afterload. This renders the conventional load-dependent parameters unreliable as parameters of contractility.[12] Therefore, *in vivo* cardiac performance was measured by both load-dependent and load-independent parameters derived from pressure–volume loops, obtained *in vivo* using miniaturized pressure-conductance catheterization, as previously described.[2] Briefly, mice were anesthetized with a mixture of urethane (1200 mg/kg)–α-chloralose (50 mg/kg) and were mechanically ventilated. A pressure-conductance catheter (1.4-Fr, SPR-839; Millar Instruments, Houston, TX, USA) was inserted in the left ventricle (LV), via the carotid artery. After stabilization, steady-state measurements were recorded. Heart rate (HR), end-diastolic volume (V_{ed}) as a parameter for preload, arterial elastance (E_a) as a parameter for afterload, the maximum and minimum rate of pressure development (dP/dt_{max}, dP/dt_{min}), the time constant of relaxation during isovolumetric diastole (τ), and cardiac output (CO) were derived. Load-independent parameters of contractility [end-systolic elastance (E_{es}), preload-recruitable stroke work (PRSW), and the slope of the end-diastolic pressure–volume relationship (EDPVR)] were obtained by decreasing LV preload (temporary occlusion of the inferior vena cava). EDPVR was calculated using a linear fit (EDPVR linear) and using an exponential fit (EDPVR exp). Ventriculo-arterial coupling was determined by the relationship between E_{es} and E_a (E_{es}/E_a). Because small differences in contractility are often indiscernible in basal conditions, cardiac reserve was tested by catecholamine administration. Therefore, stepwise increasing doses of dobutamine (0–10 μg/kg/min) were administered by continuous infusion in the jugular vein, after recording baseline haemodynamic parameters. Absolute volume was calculated using the hypertonic saline and cuvette calibration method.[2]

2.3.2 Blood–pressure telemetry

In a subgroup of 24 week old mice, miniaturized telemetry devices (Datascience Corp) were implanted as previously described[13] and mice were left to recover for at least 1 week before recordings were done. Pulse pressure (PP) and mean arterial blood pressure (MABP) were measured, derived from blood pressure signals sampled at 2000 Hz (Notocord HEM 3.4 software).

2.4 Analysis of SERCA2a expression and function

Oxalate-supported Ca^{2+} uptake was measured in total cardiac homogenates under conditions that restricted Ca^{2+} uptake to the SR.[14] The maximal velocity of Ca^{2+} uptake (V_{max}), the Ca^{2+} concentration required for half-maximal activation (K_m), and the Hill coefficient (n) were calculated by non-linear regression analysis (Microcal Origin software), based on the Hill equation:

$$v = \frac{V_{max}[Ca^{2+}]^n}{K_m + [Ca^{2+}]^n}.$$

Ventricular homogenates were analysed by standard Western blotting.[14] Phosphatase activity was inhibited with (nmol/L) 25 NaF, 5 Na-EDTA, 5 $Na_4P_2O_7$, and a phosphatase inhibitor cocktail (Sigma, P2850). Equal amounts of protein were separated on 4–20% Bis-Tris gradient gels (NuPAGE, Invitrogen) and blotted onto PVDF membranes (Immobilon-P, Millipore Corp.). Membranes were probed with primary antibodies against SERCA2a,[15] PLB (A1 antibody, UBI), phosphoserine (PS16), and phosphothreonine (PT17) of PLB (Cyclacel). Phosphorylation of PLB relieves the functional inhibition of SERCA by PLB, thereby increasing the pump's affinity, without changing the maximal pumping rate. Protein kinase A (PKA) and Ca^{2+} calmodulin kinase II (CaMKII) are the physiological relevant kinases, which phosphorylate PLB. PKA is activated upon β-adrenergic stimulation and phosphorylates PLB at the serine 16 site. CaMKII is activated in the presence of high Ca^{2+} levels and/or secondary to increased intracellular cAMP levels; it phosphorylates PLB at the threonine 17 site.[16] Detection was performed using secondary antibodies coupled to alkaline phosphatase and the ECF substrate (Amersham Pharmacia Biotech).

2.5 Histology

Hearts were perfused and injected with 100 μL saline containing 0.1 mM $CdCl_2$. Afterwards, hearts were excised and embedded in Tissue Freezing medium (Leica Microsystems) and frozen in liquid N_2. Oil Red O staining of cross-sections (7 μm) from the aortic root and throughout the ventricle was used to quantify the extent of the atherosclerotic lesions in the aortic arch, respectively, coronary arteries. Sirius Red staining was used to visualize collagen. The amount of collagen was quantified as percentage Sirius Red stained area per total cardiac area.[17] A total of five images per animal were analysed to evaluate cardiac fibrosis. Haematoxylin/Eosin (H&E) staining was used for routine histological examination. The average cardiomyocyte cross-sectional area was evaluated in the subendocardial layer, the central and the subepicardial layer of the LV, on H&E-stained sections. Sixty cells were measured per heart. To quantify the relative numbers of cells with DNA fragmentation, TUNEL assay was performed in heart tissue sections using the FragEL DNA Fargmentation Detection Kit (Calbiochem), according to the protocol of the manufacturer. To determine the percentage apoptotic cells, TUNEL-positive and TUNEL-negative cells were counted. Results are expressed as number of TUNEL-positive cells/total cells × 100%. All morphometric analysis was performed blinded with the Quantimet600 Image Analyzer (Leica).

2.6 Statistical analysis

All statistical analyses were performed using Statistica 6.0 (Statsoft, Tulsa, OK, USA). Data are expressed as mean ± SD, unless otherwise specified. Differences between groups were compared by 1-way ANOVA followed by a LSD *post hoc* test. Repeated measures were compared by Repeated Measures ANOVA. Correlations were determined by the Pearson test. A value of $P < 0.05$ was considered significant.

3. Results

3.1 Biochemical analysis at 12, 24, and 36 weeks

Body weight was higher in ob/ob and DKO mice compared with WT at all ages. Glucose and insulin levels, and thus the HOMA-IR index were equally elevated in ob/ob and DKO mice. Glucose tolerance was impaired in ob/ob and DKO mice compared with that from WT. Total cholesterol levels were elevated in LDLR$^{-/-}$ and DKO mice, compared with WT and ob/ob. In LDLR$^{-/-}$ mice, total cholesterol was approximately three times higher than in WT, whereas in DKO mice total cholesterol reached even 10 times higher levels. Plasma triglycerides were significantly higher in DKO mice in comparison with WT and ob/ob, at all ages. In 36 weeks old LDLR$^{-/-}$ mice, triglyceride levels were higher (*Table 1*).

3.2 *In vivo* cardiac performance

3.2.1 Left-ventricular pressure–volume analysis

No statistical differences were observed between WT and LDLR$^{-/-}$ mice at any age, nor were there significant age-dependent haemodynamic changes in these mice (data not shown). Representative examples of pressure volume loops during preload reduction are shown in *Figure 1*. *Figure 2* summarizes the baseline *in vivo* data of the ob/ob, DKO, and WT mice.

HR in ob/ob and DKO mice was slightly lower than in WT at 36 weeks of age. Left ventricular end-diastolic volume (V_{ed}) was similar in the different genotypes at 12 weeks of age; thereafter, it decreased with age in DKO mice and increased with age in ob/ob mice. At 36 weeks, V_{ed} was significantly higher in ob/ob mice and lower in DKO mice in comparison with WT. Arterial elastance (E_a) was lower in both ob/ob and DKO mice at 12 weeks of age in comparison with WT. Whereas it remained low in ob/ob mice, it increased with age in DKO mice. From 24 weeks onwards, the difference in E_a between DKO and WT disappeared. E_a is calculated as the end-systolic pressure divided by the stroke volume. It was mainly the differential change in stroke volume (increased in ob/ob, but decreased in DKO in function of age) leading to the observed differences in E_a (data not shown). Contractility was impaired in both ob/ob and DKO mice from 24 weeks onwards, which was evidenced by a decrease of the load-independent PRSW. End-systolic elastance (E_{es}) was also lower at 24 weeks in these mice. However, in 36 weeks old DKO mice, E_{es} was not different from WT. Load-dependent dP/dt_{max} and EF (data not shown) were comparable in all groups at 24 and 36 weeks of age. Whereas early diastolic relaxation (dP/dt_{min}, τ) was similarly impaired from age 24 weeks onwards in both ob/ob and DKO mice, ventricular stiffness (EDPVR linear and EDPVR exp) was only increased in DKO mice.

Table 1 Biochemical parameters in 12, 24, and 36 weeks old WT, ob/ob, and DKO mice

	WT	LDLR$^{-/-}$	ob/ob	DKO
12 weeks	$n = 16$	$n = 14$	$n = 10$	$n = 8$
Weight (g)	23.7 ± 3.4	21.5 ± 2.9	43.3 ± 5.2*	46.6 ± 4.3*
Glucose (mM)	4.3 ± 1.8	4.3 ± 1.8	9.6 ± 3.2*	9.9 ± 1.3*
Total cholesterol (mg/dL)	63 ± 10	183 ± 46*	109 ± 35	604 ± 103*,**
Triglycerides (mg/dL)	58 ± 13	78 ± 17	61 ± 10	499 ± 238*,**
Insulin (mU/L)	384 ± 269	468 ± 164	1263 ± 494*	1384 ± 534*
HOMA-IR	73 ± 21	108 ± 21	539 ± 70*	609 ± 79*
AUC of the IPGTT ($\times 10^4$)	5.7 ± 0.88	5.6 ± 2.3	11.6 ± 3.4*	12.3 ± 5.5*
24 weeks	$n = 14$	$n = 14$	$n = 8$	$n = 14$
Weight (g)	26.5 ± 4.7	26.8 ± 3.0	59.7 ± 4.5*	57.3 ± 3.6*
Glucose (mM)	4.3 ± 0.83	4.6 ± 0.49	9.2 ± 5.3*	9.6 ± 2.0*
Total cholesterol (mg/dL)	78 ± 19	213 ± 68*	136 ± 51	584 ± 170*,**
Triglycerides (mg/dL)	43 ± 5	65 ± 20	49 ± 13	458 ± 178*,**
Insulin (mU/L)	330 ± 100	310 ± 78	1849 ± 580*	1504 ± 489*
HOMA-IR	63 ± 4	64 ± 7	756 ± 136*	642 ± 139*
AUC of the IPGTT ($\times 10^4$)	6.2 ± 1.1	6.9 ± 2.3	13.3 ± 4.4*	15.2 ± 3.0*
36 weeks	$n = 19$	$n = 14$	$n = 10$	$n = 11$
Weight (g)	28.8 ± 3.8	27.4 ± 4.1	68.9 ± 10.5*	58.7 ± 6.7*
Glucose (mM)	3.9 ± 0.85	4.2 ± 0.6	8.9 ± 5.0*	9.0 ± 4.2*
Total cholesterol (mg/dL)	57 ± 13	269 ± 110*	94 ± 23	422 ± 154*,**
Triglycerides (mg/dL)	49 ± 11	114 ± 17*	52 ± 13	497 ± 368*,**
Insulin (mU/L)	366 ± 149	364 ± 289	1613 ± 523*	1402 ± 640*
HOMA-IR	63 ± 5	67.5 ± 8.0	638 ± 116*	561 ± 119*
AUC of the IPGTT ($\times 10^4$)	5.6 ± 1.9	5.8 ± 1.7	8.0 ± 3.4	9.2 ± 3.8*

HOMA-IR indicates homeostasis model assessment; AUC, area under the curve; IPGTT, intraperitoneal glucose tolerance test.
*$P < 0.05$ vs. WT.
**$P < 0.05$ vs. ob/ob.

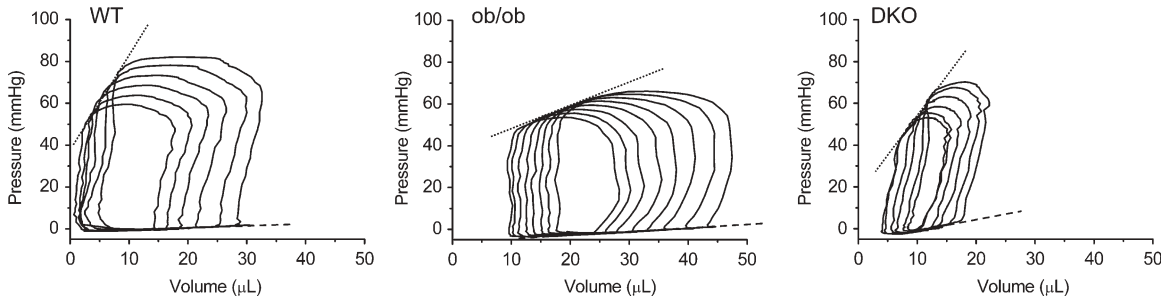

Figure 1 Representative examples of left ventricular pressure–volume loops during caval occlusion. Dotted lines represent the end-systolic pressure–volume relationship with slope E_{es} (index for systolic contractility and stiffness); dashed lines represent the end-diastolic pressure–volume relationship (EDPVR linear), the slope of which is an index of diastolic stiffness. The ob/ob mouse is characterized by large stroke volumes and large V_{ed} and a depression of the E_{es}. In DKO mice, a leftward shift and steep slope of the end-systolic pressure–volume relationship and small stroke volumes and low V_{ed} are observed. Also the slope EDPVR was steeper in these mice.

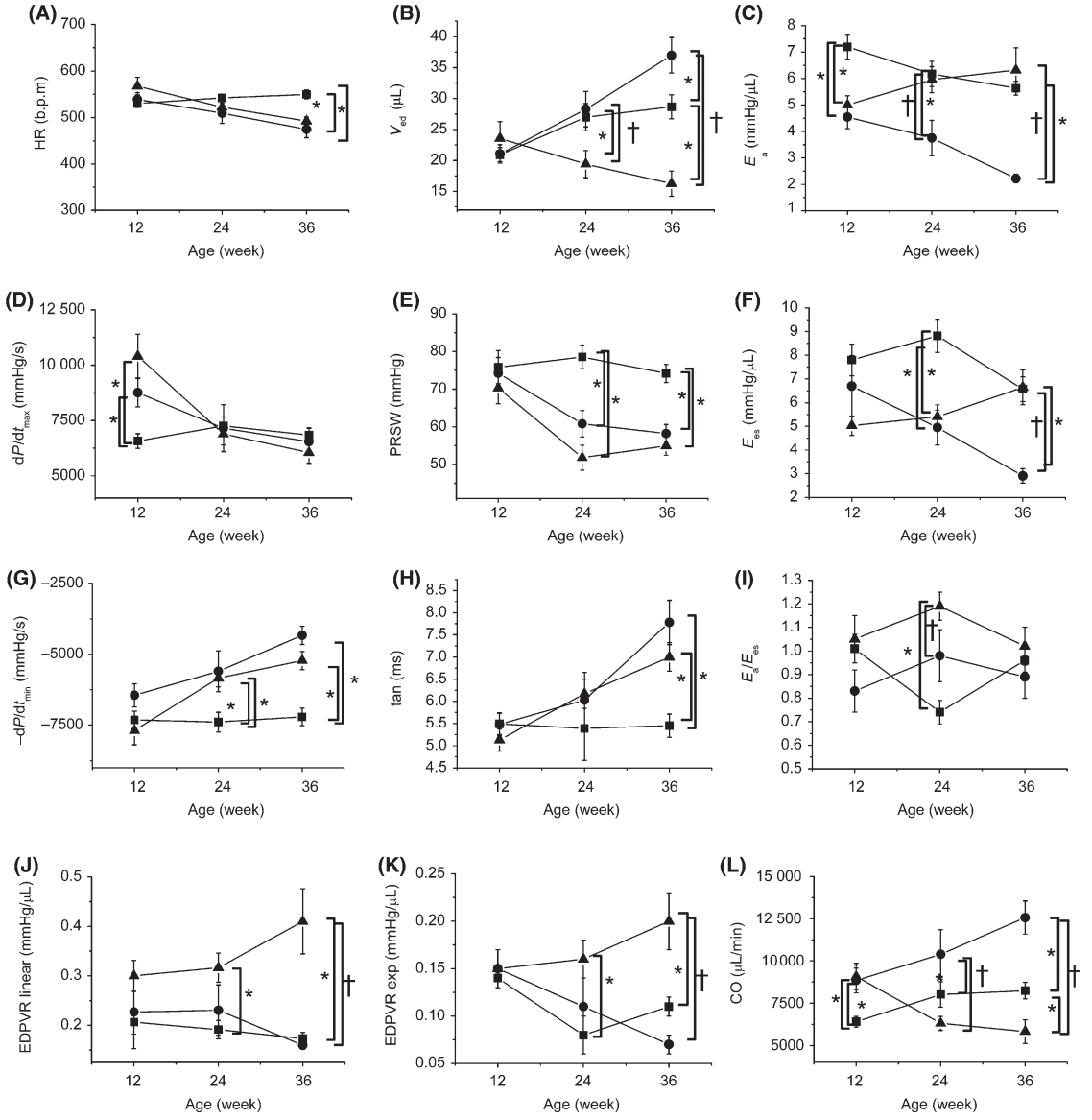

Figure 2 Baseline haemodynamic parameters. (*A*) Heart rate (HR), (*B*) end-diastolic volume (V_{ed}), (*C*) arterial elastance (E_a), (*D*) dP/dt_{max}, (*E*) preload-recruitable stroke work (PRSW), (*F*) end-systolic elastance (E_{es}), (*G*) dP/dt_{min}, (*H*) τ, (*I*) ratio E_a/E_{es}, (*J*) end-diastolic pressure volume relationship fitted linearly (EDPVR linear), (*K*) end-diastolic pressure volume relationship fitted exponentially (EDPVR exp), and (*L*) cardiac output (CO) in WT (filled square), ob/ob (filled circle), and DKO (filled triangle) mice of 12, 24, and 36 weeks of age. Data are mean ± SEM. $^*P < 0.05$ vs. WT, $^\dagger P < 0.05$ vs. ob/ob.

Ventriculo-arterial stiffening (E_a/E_{es}) was higher in DKO mice in comparison with ob/ob and WT at an age of 24 weeks. At 36 weeks, there were no significant differences anymore. CO was significantly higher in ob/ob and DKO mice at 12 weeks of age. Whereas CO decreased in DKO mice with age, it increased in ob/ob mice.

Cardiac reserve was measured during administration of stepwise incremental doses of dobutamine (*Figure 3*). Two DKO mice died at a dose of 3 μg/kg/min. These animals were excluded for the repeated measures analysis. A positive chronotropic (HR), inotropic (PRSW), and lusitropic (dP/dt_{min}) response was observed in WT mice upon β-stimulation. Inotropic and lusitropic parameters increased less in ob/ob and DKO mice than in WT, however with a normal chronotropic response. Interestingly, whereas both ob/ob and DKO mice showed a severely impaired cardiac reserve, only in DKO mice PRSW and CO did not increase further at the highest doses, even tended to decrease.

3.2.2 Blood-pressure telemetry

PP was significantly higher in ob/ob and DKO mice (33.5 ± 1.4, respectively. 32.2 ± 1.0 mmHg) when compared to WT (24.9 ± 0.9 mmHg) and $LDLR^{-/-}$ mice (24.9 ± 1.2 mmHg). MABP was 101.8 ± 1.1 mmHg in WT, and was significantly higher in $LDLR^{-/-}$ (111 ± 1.2 mmHg), ob/ob (108.7 ± 1.8 mmHg), and DKO mice (111.4 ± 1.2 mmHg).

3.3 SERCA2a expression and activity

The averaged curves of Ca^{2+} reuptake in fragmented SR from 36 weeks old animals are presented in *Figure 4A*. Representative examples of western blots of ventricular SERCA2a, PLB, PS16, and PT17 in WT, ob/ob, and DKO mice at 12 and 36 weeks are given in *Figure 4B* and *C*. Figure *4D–G* summarizes the results after analysis. No statistical differences were observed between WT and LDLR −/− mice (data not shown).

At 12 weeks of age, increased SERCA2a levels but unchanged expression of PLB were observed in ob/ob and DKO mice. PLB serine 16 was relatively less phosphorylated, indicating a stronger inhibition of the Ca^{2+} pump. The combination of these factors resulted in a comparable SR Ca^{2+} reuptake in both ob/ob and DKO mice vs. WT (*Table 2*). At older ages, the PLB/SERCA2a ratio is normalized. The fraction of PLB phosphorylated on serine 16 remained lower but the fraction phosphorylated on threonine 17 increased significantly with age in both ob/ob and DKO mice. However, this increase could not overcome the effect of a lower PLB phosphorylation level on Serine 16, since Ca^{2+} reuptake experiments revealed a significantly lower apparent Ca^{2+} affinity of SERCA2a (i.e. a higher K_m value) in ob/ob and DKO mice at 24 and 36 weeks of age (*Table 2*). The Hill coefficient was lower in DKO mice compared to WT at 36 weeks of age (*Table 2*).

3.4 Histology

As shown in *Figure 5A*, heart weight was significantly higher in ob/ob mice than in WT at 12, 24, and 36 weeks of age, with heart weight in DKO taking intermediary positions. Myocyte diameters of both ob/ob and DKO mice were significantly larger in comparison with WT (*Figure 5B*).

ob/ob and DKO mice showed markedly elevated apoptosis in comparison with WT mice (*Figure 5C*). At an age of 36 weeks, the level of apoptosis in DKO mice exceeded that in ob/ob mice.

Whereas the area of the red-staining collagen was comparable in WT and ob/ob mice at all ages studied, it increased with age in DKO mice (*Figure 5D*). From an age

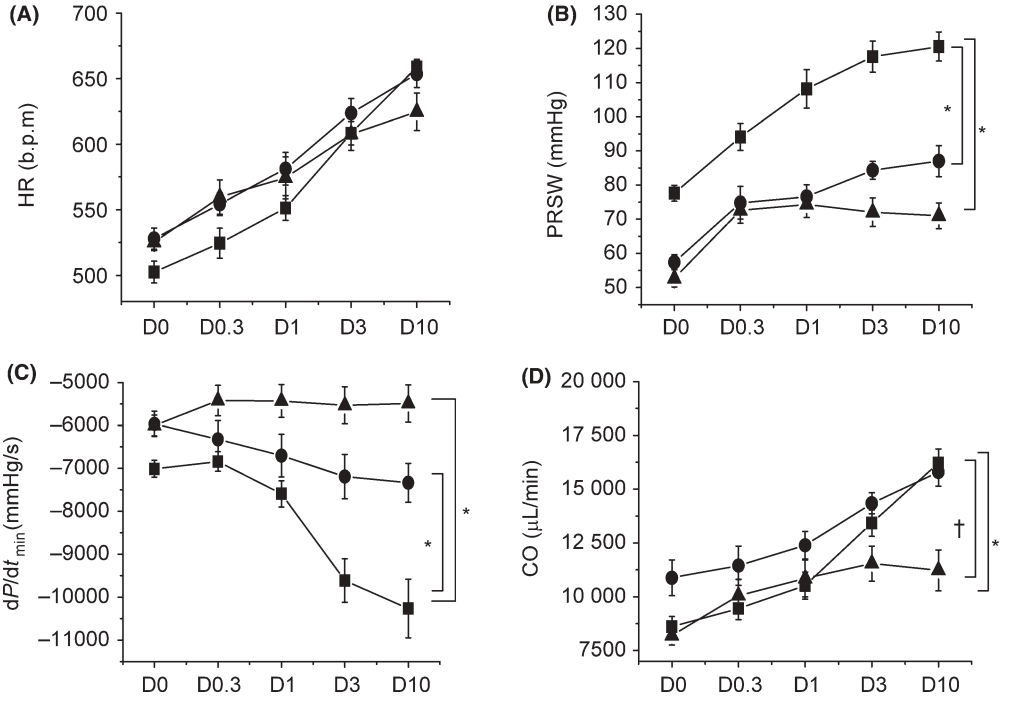

Figure 3 Cardiac performance during beta-adrenergic stimulation in 24 weeks old mice. Incremental doses of dobutamine (D0–D10 μg/kg/min) were administered by continuous infusion to test cardiac reserve during stress. Dose-response curve for (*A*) heart rate (HR), (*B*) preload-recruitable stroke work (PRSW), (*C*) dP/dt_{min}, and (*D*) cardiac output (CO) in WT (filled square), ob/ob (filled circle), and DKO (filled triangle) mice. Whereas the chronotropic response was normal, ob/ob and DKO mice displayed an impaired inotropic and lusitropic response during dobutamine-infusion, as outlined by, respectively, PRSW and dP/dt_{min}. Data are mean ± SEM. $^*P < 0.05$ vs. WT, $^\dagger P < 0.05$ vs. ob/ob.

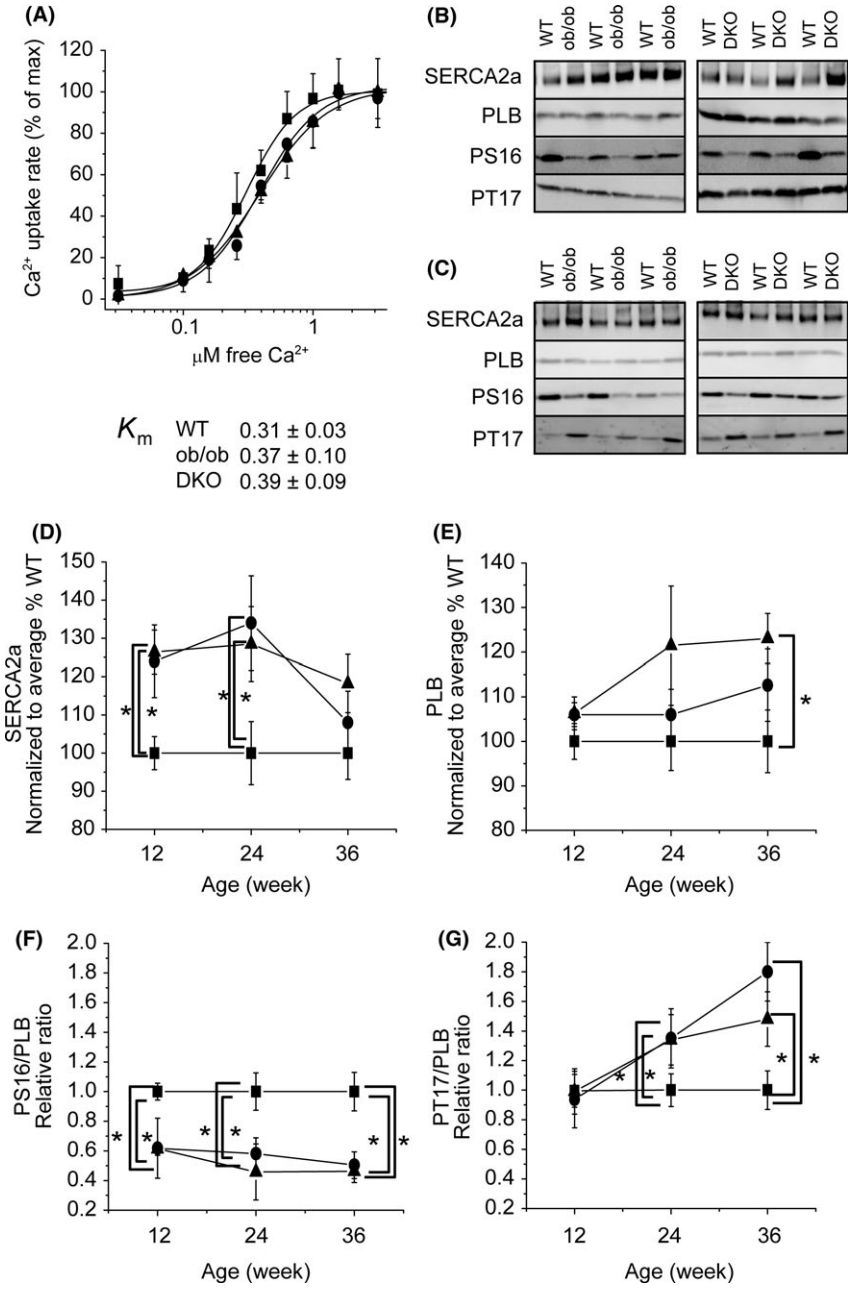

Figure 4 Analysis of the SR Ca^{2+} reuptake. (*A*) Oxalate supported Ca^{2+} uptake measurements in 36 weeks old WT (filled square), ob/ob (filled circle), and DKO (filled triangle) mice. Ca^{2+} uptake rates are normalized to the maximal uptake rate of the group. (*B* and *C*) Representative examples of western blots of total ventricular homogenates. Blots were probed with antibodies to SERCA2a, PLB, PLB phosphorylated on Serine 16 (PS16) and PLB phosphorylated on Threonine 17 (PT17) in mice of 12 (B) and 36 (C) weeks of age. (*D*–*G*) The graphs show the relative expression levels obtained by western blots. Experiments were performed in triplicate ($n = 6$ for each group). Data are presented as mean ± SEM. * $P < 0.05$ vs. WT.

of 24 weeks onwards, collagen content was significantly higher in DKO mice, compared with the WT and ob/ob.

No atherosclerotic lesions were detected in the aorta of C57BL6/J and ob/ob mice at any age, and in $LDLR^{-/-}$ mice they were only very small (even at 36 weeks of age) (always less than 0.01 mm^3). *Figure 5E* shows representative oil red O-stained cross-sections of the aortic root of DKO mice at 12, 24, and 36 weeks. In 12 weeks old DKO mice, lesions were small fatty streaks. Plaque volumes increased from 0.008 ± 0.004 mm^3 at 12 weeks to 0.081 ± 0.049 mm^3 at 24 weeks and 0.156 ± 0.020 mm^3 at 36 weeks. Atherosclerotic plaque volume in the aortic arch of DKO mice was positively correlated with arterial elastance, a parameter for afterload ($R = 0.69$; $P < 0.05$) (*Figure 5F*). No atherosclerotic lesions were found in epicardial and intramyocardial coronary arteries.

4. Discussion

This work provides evidence that left ventricular relaxation and contractility when assessed with load-independent parameters are impaired in mice with abdominal obesity and type II diabetes. SERCA2a activity paralleled the *in vivo* findings of relaxation and contractility. Ventricular-vascular stiffening and signs of deterioration of the cardiac reserve after β-adrenergic stimulation were only observed

when atherogenic dyslipidaemia was superimposed on an obesity/diabetes background. This was accompanied by increasing left ventricular fibrosis. These results offer new insights into the role of dyslipidaemia in the pathogenesis of diabetes/obesity-associated cardiovascular disease.

4.1 Atherogenic dyslipidaemia superimposed on obesity and type II diabetes does not further aggravate systolic and early diastolic dysfunction in mice

Reduced PRSW indicates impaired contractility in ob/ob and DKO mice. The steepness of the end-systolic pressure–volume relationship (E_{es}) in DKO mice is not due to improved myocardial function but instead to small chamber volumes (V_{ed}) and hypertrophy.[18] Also the unchanged values of dP/dt_{max} and ejection fraction in DKO mice vs. controls in the presence of concentric hypertrophy indicate a substantial dysfunction, since the subnormal shortening of extra parallel sarcomeres may overestimate these parameters.[19,20] In ob/ob mice, the preserved dP/dt_{max} and EF are attributable to, respectively, a high preload and a low afterload.

Contractility (PRSW) and early relaxation (dP/dt_{min}) decreased in a comparable way in ob/ob and DKO mice from an age of 24 weeks onwards. In other words, the dyslipidaemia superimposed on obesity and insulin resistance, characterizing the DKO mouse model, does not alter *in vivo* contractility and relaxation. Besides the possible involvement of other essential parameters of the contractile protein apparatus responsible for impaired function, we focused on the contribution of cardiac myocyte apoptosis and SR Ca^{2+} reuptake capacity in these mice. Cardiac myocyte apoptosis, even at low levels, is well recognized as an important step in the development of heart failure. Because increased apoptosis was already evident at an age of 12 weeks in both ob/ob and DKO mice, our findings suggest that this might trigger cardiac dysfunction. The SR Ca^{2+} reuptake activity paralleled the *in vivo* functional measurements. Indeed, SERCA2a affinity for Ca^{2+} was reduced to the same extent at all ages in ob/ob and DKO mice, indicating that also for this aspect, dyslipidaemia does not have an additional impact. On the other hand, the Hill coefficient was lower in the DKO mice, suggesting a possible role for dyslipidaemia in the cooperativity between Ca^{2+} ions and the SERCA2a molecule. However, the alterations in Hill-coefficient apparently do not have major influences on *in vivo* cardiac contractile performance in DKO mice. Thus, despite this possible interaction, dyslipidaemia does not seem to have an important role in the

Table 2 Oxalate-supported Ca^{2+} reuptake measurements in 12, 24, and 36 weeks old WT, ob/ob, and DKO mice

	WT	ob/ob	DKO
12 weeks			
V_{max}	45.1 ± 24.0	56.7 ± 25.2	53.8 ± 16.2
K_m	0.34 ± 0.10	0.37 ± 0.08	0.38 ± 0.12
Hill	2.03 ± 0.49	1.83 ± 0.57	1.86 ± 0.90
24 weeks			
V_{max}	45.3 ± 12.2	50.2 ± 13.2	47.7 ± 17.5
K_m	0.33 ± 0.04	0.39 ± 0.06*	0.39 ± 0.03*
Hill	2.24 ± 0.44	1.97 ± 0.26	1.96 ± 0.18
36 weeks			
V_{max}	36.5 ± 4.8	43.4 ± 17.3	41.9 ± 10.8
K_m	0.31 ± 0.03	0.37 ± 0.10*	0.39 ± 0.09*
Hill	2.1 ± 0.19	1.95 ± 0.61	1.67 ± 0.37*

Maximal Ca^{2+} uptake rate in nmol Ca^{2+}/mg protein/min (V_{max}), apparent Ca^{2+} affinity in μM (K_m), and the Hill coefficient are summarized for WT, ob/ob, and DKO mice of 12, 24, and 36 weeks of age. Experiments were performed in triplicate ($n = 6$ for each group).
*$P < 0.05$ vs. WT.

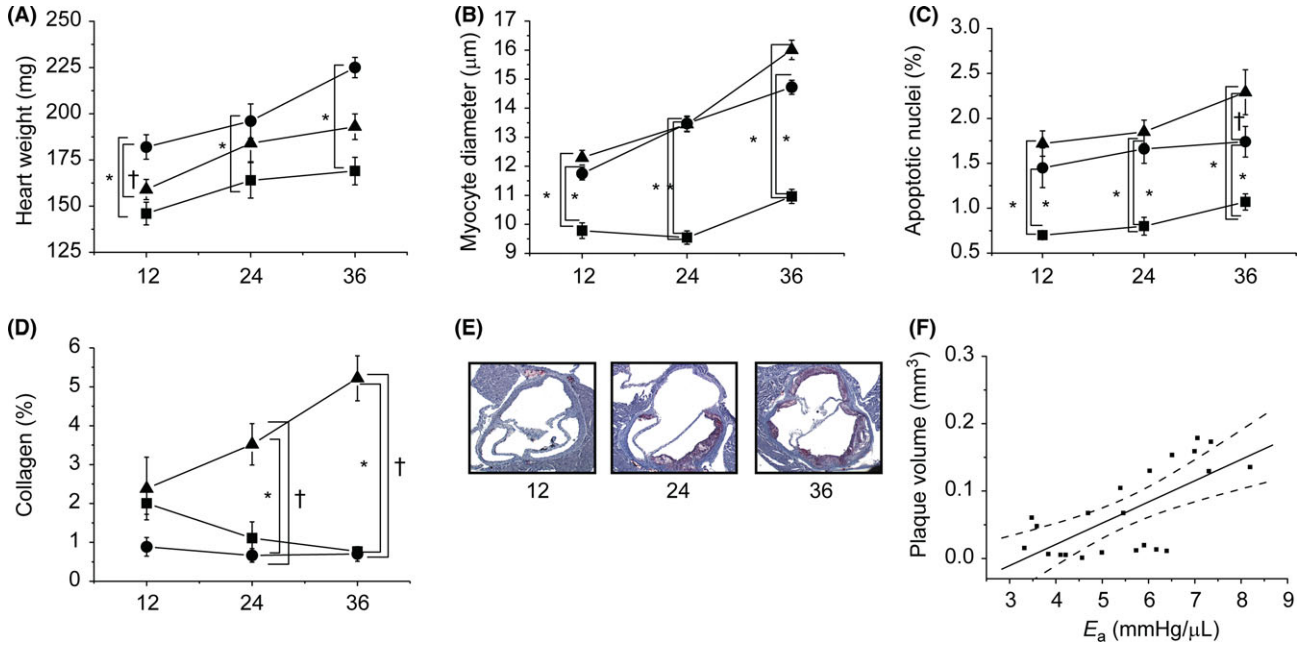

Figure 5 Histology. (*A*) Heart weight, (*B*) myocyte diameters, (*C*) levels of apoptosis, and (*D*) collagen accumulation in 12, 24, and 36 weeks old WT (filled square), ob/ob (filled circle), and DKO (filled triangle) mice. Data are presented as mean ± SEM ($n = 5$ for each group). *$P < 0.05$ vs. WT, †$P < 0.05$ vs. ob/ob. (*E*) Representative cross-sections of aortic arch from DKO mice at 12, 24, and 36 weeks. (*F*) Correlation of plaque volume with arterial elastance (E_a), as parameter for afterload.

development of contractile dysfunction related to impaired SR function in type II DM.

Our study revealed that the reduced SERCA2a activity observed in 24 and 36 weeks old ob/ob and DKO mice results mainly from altered regulation and phosphorylation state of PLB. A significantly decreased Serine 16 phosphorylation level was detected at all ages, whereas the phosphorylation level on Threonine 17 was normal at 12 weeks but afterwards increased with age. At baseline conditions, Serine 16 phosphorylation is thought to play a more dominant role in controlling SERCA2 activity than on Threonine 17.[21] It remains to be elucidated which components of the phosphorylation pathways are defective in ob/ob and DKO mice. Impaired PKA activity was postulated to result from leptin deficiency, leading to decreased Serine 16 phosphorylation.[22] Increased CaMKII activity results from increased cytosolic Ca^{2+} concentrations and may lead to increased Threonine 17 phosphorylation.[21] Although no study to date was performed regarding intracellular Ca^{2+} levels in ob/ob or DKO mice, we demonstrated in both mouse models the development of cardiac hypertrophy. Interestingly, numerous studies indicate that cardiac hypertrophy is associated with elevated intracellular Ca^{2+}.[23,24] Besides altered PKA and CaMKII activity, the role of phosphatases in controlling the phosphorylation status of PLB may not be underestimated. Recently, it was shown that phosphatases might play a crucial role in hypertrophic cardiomyopathy.[25,26]

4.2 Atherogenic dyslipidaemia superimposed on obesity and type II diabetes increases ventricular stiffness in leptin-deficient mice

The most important difference in the haemodynamic profile between ob/ob and DKO mice lies in the parameters defining stiffness/compliance. The three parameters defining stiffness using pressure–volume relationships are the end-systolic elastance (E_{es}), the arterial elastance (E_a), and the slope of the EDPVR. It was previously reported that ventricular systolic and diastolic stiffening increase in tandem with artery stiffening, which is likely linked to the coupling of the heart and the vascular system.[27] Indeed, the DKO mouse displays marked increases in both end-systolic and arterial elastance in comparison to ob/ob mice. The diastolic pressure–volume relation is also steeper in the DKO mice. We already remarked that the steepness of the E_{es} in DKO mice does not reflect improved myocardial function but instead is related to the small chamber volumes (V_{ed}) and hypertrophy.[18] The increase in E_a in DKO mice in function of age might, at least partially, be related to atherosclerotic plaque formation. We observed, in this study, a positive correlation between atherosclerotic plaque volume and arterial elastance in DKO mice. In ob/ob mice, E_a was lower compared to WT at all ages. E_a is linearly related to both total peripheral resistance (R) and the reciprocal of the compliance ($1/C$).[28] The low E_a in ob/ob mice seems to be in agreement with studies in massively obese patients without signs of hypertension exhibiting reduced peripheral resistance and normal arterial compliance.[29] When massive obesity is combined with atherosclerosis, the net result on arterial elastance is more difficult to predict. It is tempting to speculate that the atherosclerotic lesions in these mice might decrease aortic compliance to such an extent, that it counteracts the reduced E_a observed in ob/ob mice. However, whereas plaque volume doubled from age 24 to 36 weeks, there was only a modest (10%) increase in E_a. This is in agreement with the findings of Segers *et al.*,[28] who reported that the sensitivity of E_a to $1/C$ is three times lower than to R. Hence, the compliance term only contributes for a minor part to changes in E_a. The telemetric measurements are in line with these findings. In both ob/ob and DKO mice, a higher PP was observed. PP arises from the interaction of cardiac ejection (stroke volume) and the properties of the arterial circulation.[30] A higher PP in ob/ob mice might be attributed to a higher stroke volume; but in DKO mice, stroke volume is normal, thus the higher PP is likely to be generated by an increased stiffness of the major arteries, in line with the increased E_a. Finally, the steepness of the EDPVR in DKO mice could be related to the increase in intramyocardial collagen accumulation (*Figure 5C*). No deposition of collagen, with concomitant increased passive stiffness was detected in ob/ob mice.

The age-related rise in E_a in the DKO mice was associated with a modest rise in ventricular E_{es}, meaning that simultaneous ventricular-vascular stiffening maintained an equal E_a/E_{es} ratio. In comparison with the ob/ob mice, both parameters were significantly elevated from an age of 24 weeks. One could anticipate that it would be beneficial when the E_a/E_{es} ratio is maintained; however, important consequences may arise in the cardiac response to increased filling volumes, since a stiff heart-arterial system generates more systolic pressure change for a given change in ventricular volume. A higher pressure will be generated, but a smaller ejected stroke volume will be achieved. This means that although both E_{es} and E_a/E_{es} ratio are normal in DKO mice, the way the heart responds to preload alteration is changed.

Interestingly, Hundley *et al.*[31] reported that such 'coupled stiffening' contributes to stress intolerance, a finding which is confirmed by our study. DKO mice displayed a worse contractile reserve upon dobutamine-stimulation in comparison with ob/ob mice.

5. Conclusion

The pattern of left ventricular dysfunction development in the leptin-deficient ob/ob mouse—as a model of type II diabetes—and in the DKO ($LDLR^{-/-}$;ob/ob) mouse—as a model featuring several characteristics of the metabolic syndrome (including obesity, type II diabetes, hyperlipidaemia, and atherosclerosis)—can clearly be differentiated. Left ventricular contractility and early diastolic relaxation are impaired in both obese diabetic mouse models, and are related to increased apoptosis and defective SR Ca^{2+} reuptake. The additional features of the metabolic syndrome (apart from obesity and insulin resistance) seem to be responsible for a differential pattern of remodelling, for an increased passive ventricular stiffness, and intramyocardial fibrosis. Arterial elastance is lower in obese diabetic mice, but this is counteracted by the atherosclerotic dyslipidaemia at 24 and 36 weeks, in parallel with the development of atherosclerotic lesions. The global cardiac phenotypic outcome in the DKO mice model of the metabolic syndrome is worse than in the ob/ob mouse model of type II diabetes.

Acknowledgments

We thank Hilde Bernar, Erik Verbeken, Melissa Swinnen, Davy Vanhoutte, and Birgit den Adel for excellent technical assistance.

Funding

A.V.D.B. received a pre-doctoral bursary of the Institute for the Promotion of Innovation through Science and Technology in Flanders (IWT-SB/23231). P.V. is a post-doctoral fellow of the Research Fund K.U.Leuven. F.D. is Aspirant of the Fonds National de la Recherche Scientifique (FNRS). This research was supported by funds from a Research Programme of the Research Foundation—Flanders (FWO—Vlaanderen, G.0381.05 and G.0276.04 N), by the Vascular Biology Program of FWO, and from an Onderzoeksfonds K.U.Leuven/Research Fund K.U.Leuven (OT/05/55) and Interuniversity Attraction Pole (PAI-P6/55).

Conflict of interest: none declared.

References

1. Fang ZY, Prins JB, Marwick TH. Diabetic cardiomyopathy: evidence, mechanisms, and therapeutic implications. *Endocr Rev* 2004;**25**:543–567.
2. Van Den Bergh A, Flameng W, Herijgers P. Type II diabetic mice exhibit contractile dysfunction but maintain cardiac output by favourable loading conditions. *Eur J Heart Fail* 2006;**8**:777–783.
3. Semeniuk LM, Kryski AJ, Severson DL. Echocardiographic assessment of cardiac function in diabetic db/db and transgenic db/db-hGLUT4 mice. *Am J Physiol Heart Circ Physiol* 2002;**283**:H976–H982.
4. Third Report of the National Cholesterol Education Program (NCEP) Expert Panel on Detection, Evaluation, and Treatment of High Blood Cholesterol in Adults (Adult Treatment Panel III) final report. *Circulation* 2002;**106**:3143–31421.
5. Grundy SM, Cleeman JI, Daniels SR, Donato KA, Eckel RH, Franklin BA, Gordon DJ, Krauss RM, Savage PJ, Smith SC Jr, Spertus JA, Costa F. Diagnosis and management of the metabolic syndrome: an American Heart Association/National Heart, Lung, and Blood Institute Scientific Statement. *Circulation* 2005;**112**:2735–2752.
6. Mertens A, Verhamme P, Bielicki JK, Phillips MC, Quarck R, Verreth W, Stengel D, Ninio E, Navab M, Mackness B, Mackness M, Holvoet P. Increased low-density lipoprotein oxidation and impaired high-density lipoprotein antioxidant defense are associated with increased macrophage homing and atherosclerosis in dyslipidemic obese mice: LCAT gene transfer decreases atherosclerosis. *Circulation* 2003;**107**:1640–1646.
7. Verreth W, De Keyzer D, Pelat M, Verhamme P, Ganame J, Bielicki JK, Mertens A, Quarck R, Benhabiles N, Marguerie G, Mackness B, Mackness M, Ninio E, Herregods MC, Balligand JL, Holvoet P. Weight loss-associated induction of peroxisome proliferator-activated receptor-alpha and peroxisome proliferator-activated receptor-gamma correlate with reduced atherosclerosis and improved cardiovascular function in obese insulin-resistant mice. *Circulation* 2004;**110**:3259–3269.
8. Li SY, Yang X, Ceylan-Isik AF, Du M, Sreejayan N, Ren J. Cardiac contractile dysfunction in Lep/Lep obesity is accompanied by NADPH oxidase activation, oxidative modification of sarco(endo)plasmic reticulum Ca(2+)-ATPase and myosin heavy chain isozyme switch. *Diabetologia* 2006;**49**:1434–1446.
9. Barouch LA, Gao D, Chen L, Miller KL, Xu W, Phan AC, Kittleson MM, Minhas KM, Berkowitz DE, Wei C, Hare JM. Cardiac myocyte apoptosis is associated with increased DNA damage and decreased survival in murine models of obesity. *Circ Res* 2006;**98**:119–124.
10. Vangheluwe P, Raeymaekers L, Dode L, Wuytack F. Modulating sarco(endo)plasmic reticulum Ca^{2+} ATPase 2 (SERCA2) activity: cell biological implications. *Cell Calcium* 2005;**38**:291–302.
11. Huang Y, Walker KE, Hanley F, Narula J, Houser SR, Tulenko TN. Cardiac systolic and diastolic dysfunction after a cholesterol-rich diet. *Circulation* 2004;**109**:97–102.
12. Carabello BA. Evolution of the study of left ventricular function: everything old is new again. *Circulation* 2002;**105**:2701–2703.
13. Pelat M, Dessy C, Massion P, Desager JP, Feron O, Balligand JL. Rosuvastatin decreases caveolin-1 and improves nitric oxide-dependent heart rate and blood pressure variability in apolipoprotein $E^{-/-}$ mice *in vivo*. *Circulation* 2003;**107**:2480–2486.
14. Verheyen M, Heymans S, Antoons G, Reed T, Periasamy M, Awede B, Lebacq J, Vangheluwe P, Dewerchin M, Collen D, Sipido K, Carmeliet P, Wuytack F. Replacement of the muscle-specific sarcoplasmic reticulum Ca^{2+}-ATPase isoform SERCA2a by the nonmuscle SERCA2b homologue causes mild concentric hypertrophy and impairs contraction-relaxation of the heart. *Circ Res* 2001;**89**:838–846.
15. Eggermont JA, Wuytack F, Verbist J, Casteels R. Expression of endoplasmic-reticulum $Ca^{2(+)}$-pump isoforms and of phospholamban in pig smooth-muscle tissues. *Biochem J* 1990;**271**:649–653.
16. MacLennan DH, Kranias EG. Phospholamban: a crucial regulator of cardiac contractility. *Nat Rev Mol Cell Biol* 2003;**4**:566–577.
17. Heymans S, Lupu F, Terclavers S, Vanwetswinkel B, Herbert JM, Baker A, Collen D, Carmeliet P, Moons L. Loss or inhibition of uPA or MMP-9 attenuates LV remodeling and dysfunction after acute pressure overload in mice. *Am J Pathol* 2005;**166**:15–25.
18. Kass DA, Maughan WL. From 'Emax' to pressure-volume relations: a broader view. *Circulation* 1988;**77**:1203–1212.
19. De Simone G, Devereux RB, Celentano A, Roman MJ. Left ventricular chamber and wall mechanics in the presence of concentric geometry. *J Hypertens* 1999;**17**:1001–1006.
20. Shimizu G, Zile MR, Blaustein AS, Gaasch WH. Left ventricular chamber filling and midwall fiber lengthening in patients with left ventricular hypertrophy: overestimation of fiber velocities by conventional midwall measurements. *Circulation* 1985;**71**:266–272.
21. Mattiazzi A, Mundina-Weilenmann C, Vittone L, Said M, Kranias EG. The importance of the Thr17 residue of phospholamban as a phosphorylation site under physiological and pathological conditions. *Braz J Med Biol Res* 2006;**39**:563–572.
22. Minhas KM, Khan SA, Raju SV, Phan AC, Gonzalez DR, Skaf MW, Lee K, Tejani AD, Saliaris AP, Barouch LA, O'Donnell CP, Emala CW, Berkowitz DE, Hare JM. Leptin repletion restores depressed {beta}-adrenergic contractility in ob/ob mice independently of cardiac hypertrophy. *J Physiol* 2005;**565**:463–474.
23. Perreault CL, Shannon RP, Shen YT, Vatner SF, Morgan JP. Excitation-contraction coupling in isolated myocardium from dogs with compensated left ventricular hypertrophy. *Am J Physiol* 1994;**266**:H2436–H2442.
24. Bustamante JO, Ruknudin A, Sachs F. Stretch-activated channels in heart cells: relevance to cardiac hypertrophy. *J Cardiovasc Pharmacol* 1991;**17**(Suppl. 2):S110–S113.
25. Molkentin JD, Lu JR, Antos CL, Markham B, Richardson J, Robbins J, Grant SR, Olson EN. A calcineurin-dependent transcriptional pathway for cardiac hypertrophy. *Cell* 1998;**93**:215–228.
26. Dolmetsch RE, Lewis RS, Goodnow CC, Healy JI. Differential activation of transcription factors induced by Ca^{2+} response amplitude and duration. *Nature* 1997;**386**:855–858.
27. Chen CH, Nakayama M, Nevo E, Fetics BJ, Maughan WL, Kass DA. Coupled systolic-ventricular and vascular stiffening with age: implications for pressure regulation and cardiac reserve in the elderly. *J Am Coll Cardiol* 1998;**32**:1221–1227.
28. Segers P, Stergiopulos N, Westerhof N. Relation of effective arterial elastance to arterial system properties. *Am J Physiol Heart Circ Physiol* 2002;**282**:H1041–H1046.
29. Herrera MF, Deitel M. Cardiac function in massively obese patients and the effect of weight loss. *Can J Surg* 1991;**34**:431–434.
30. Dart AM, Kingwell BA. Pulse pressure—a review of mechanisms and clinical relevance. *J Am Coll Cardiol* 2001;**37**:975–984.
31. Hundley WG, Kitzman DW, Morgan TM, Hamilton CA, Darty SN, Stewart KP, Herrington DM, Link KM, Little WC. Cardiac cycle-dependent changes in aortic area and distensibility are reduced in older patients with isolated diastolic heart failure and correlate with exercise intolerance. *J Am Coll Cardiol* 2001;**38**:796–802.